Electronic and structural dynamics during the switching of the photomagnetic complex [Fe(L222N5)(CN)2]

Serhane Zerdane, Eric Collet, X. Dong, Samir F. F Matar, Hongfeng F. Wang, Cédric Desplanches, Guillaume Chastanet, Matthieu Chollet, James M. M Glownia, Henrik T. Lemke, et al.

Electronic and structural dynamics during the switching of the photomagnetic complex $[Fe(L_{222}N_5)(CN)_2]$

S. Zerdane,[a] E. Collet,*[a] X. Dong,[a] S. F. Matar, [b,c] H. F. Wang,[b] C. Desplanches,[b] G. Chastanet,[b] M. Chollet,[d] J. M. Glownia,[d] H.T. Lemke,[d,e] M. Lorenc,[a] M. Cammarata,*[a]

Fast and Ferrous!

! We study ultrafast light-induced excited spin-state trapping in the photomagnetic complex $[Fe(L_{222}N_5)(CN)_2]$ by femtosecond optical and X-ray absorption studies. The study, supported by theoretical calculations, reveals different switching pathways involving coherent structural dynamics

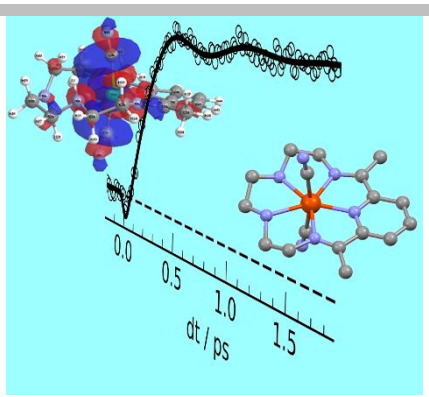

Ultrafast LIESST

S. Zerdane, E. Collet, X. Dong, S. F. Matar, H. F. Wang, C. Desplanches, G. Chastanet, M. Chollet, J. M. Glownia, H.T. Lemke, M. Lorenc, M. Cammarata,**

Page No. – ***Page No.***
Electronic and structural dynamics during the switching of the photomagnetic complex $[Fe(L_{222}N_5)(CN)_2]$

[a] S. Zerdane, E. Collet, X. Dong, M. Lorenc, M. Cammarata
Univ Rennes 1, CNRS, Institut de Physique de Rennes, UMR 6251, UBL, F-35042 Rennes, France
E-mail: eric.collet@univ-rennes1.fr, marco.cammarata@univ-rennes1.fr
[b] H. F. Wang, C. Desplanches, G. Chastanet, S. F. Matar,
CNRS, Université de Bordeaux, ICMCB, 87 avenue du Dr A. Schweitzer, Pessac, F'33608, France
[c] Lebanese German University (LGU), Sahel Alam Campus, P.O.BOX 206 Jounieh. Lebanon
[c] M. Chollet, J. M. Glownia, Henrik Lemke
LCLS, SLAC National Laboratory, Menlo Park, 94025, CA, USA.
[d] H.T. Lemke, SwissFEL, Paul Scherrer Institut, Villigen PSI 5232, Switzerland

Electronic and structural dynamics during the switching of the photomagnetic complex $[Fe(L_{222}N_5)(CN)_2]$

S. Zerdane,[a] E. Collet,*[a] X. Dong,[a] S. F. Matar, [b,c] H. F. Wang,[b] C. Desplanches,[b] G. Chastanet,[b] M. Chollet,[d] J. M. Glownia,[d] H.T. Lemke,[d,e] M. Lorenc,[a] M. Cammarata,*[a]

Abstract: The $[Fe(L_{222}N_5)(CN)_2]$ compound, where $L_{222}N_5$ refers to the macrocyclic Schiff-base ligand, 2,13-dimethyl-3,6,9,-12,18-pentaazabicyclo[12.3.1]octadeca-1(18),2,12,14,16-pentaene, is a photomagnetic Fe^{II} based coordination compound, which undergoes light-induced excited spin-state trapping (LIESST). The low spin state is hexacoordinated and the high spin state heptacoordinated. This system also serves as complex for the design of trinuclear or one-dimensional compounds made of other types of bricks with diverse coordinated metals. Here we study its ultrafast spin-state photoswitching dynamics, by combining femtosecond optical spectroscopy and femtosecond X-ray absorption measurements at the XPP station of the X-ray free-electron laser LCLS. DFT and TD-DFT calculations are used to interpret experimental findings. These studies performed in the solution phase show that LIESST in $[Fe(L_{222}N_5)(CN)_2]$ occurs on the 100 fs timescale under different types of photoexcitation. In addition, we observe coherent oscillations resulting from the structural dynamics accompanying LIESST, which were recently evidenced in more conventional octahedral $Fe^{II}N_6$ systems.

Introduction

The design of materials able to store information on the single molecule level or on assemblies of molecules is a current challenge in information technology. Among all the investigated systems, an interesting class of molecular switches are those undergoing the light-induced excited spin state trapping (LIESST) phenomenon, between low spin (LS) and high spin (HS) states. LIESST was deeply investigated in many spin-crossover materials and especially in $Fe^{II}N_6$ systems.[1] In the solid state, LIESST can be induced at low temperature by conventional techniques since the photoinduced HS state is long-lived.[2] At high temperature, LIESST is transient and can be studied by time-resolved techniques, down to the femtosecond timescale, in solution[3] or in solids[4]. Several studies using optical spectroscopy, X-ray spectroscopy or IR spectroscopy demonstrated that LIESST occurs on the 100 fs timescale from the initial photoexcited state (MLCT, LMCT or d-d) to the HS state. Very recent studies focused on the ultrafast structural dynamics accompanying LIESST. Between the two spin states, an important structural reorganization occurs: the population of antibonding orbitals in the HS state increases the equilibrium Fe-ligand distance. However, as the system reaches the HS potential at a position different from the equilibrium structure, a coherent structural dynamics starts, related to the activation and damping of the breathing mode, i.e. the expansion of the FeN_6 core.[3h, 4c, 4h, 5] In the Fe systems for which LIESST was investigated on femtosecond timescale, the iron is hexacoordinated in both LS and HS states with $Fe^{II}N_6$, $Fe^{II}N_4O_2$ or $Fe^{III}N_4O_2$.

In this paper we study the $[Fe(L_{222}N_5)(CN)_2]$ photomagnetic Fe^{II} coordination compound, involving the $L_{222}N_5$ macrocyclic Schiff-base ligand, 2,13-dimethyl-3,6,9,-12,18-pentaazabicyclo[12.3.1]octadeca-1(18),2,12,14,16-pentaene (Fig. 1). This complex was originally synthesized by Nelson et al. and was found to be in the low-spin state at room temperature.[6] $[Fe(L_{222}N_5)(CN)_2]$ also serves as linker for the design of trinuclear molecular complexes or one-dimensional compounds made of other types of coordinated metal bricks.[7] Its photomagnetic properties allow for example to switch “on” and “off” the magnetic interaction between the photoinduced Fe^{II} HS unit (S = 2) and the Mn^{III} ions in Mn-Fe-Mn trimers. The structure of this complex was revealed in the $[Fe(L_{222}N_5)(CN)_2]\cdot H_2O$ complex by Ababei et al, where the system is LS at 150 K. The Fe^{II} ion is then hexacoordinated (Fig. 1) with 2 cyanido ligands in axial positions (Fe-CN=1.94−1.96 Å) and 4 N atoms from the macrocyclic ligand $L_{222}N_5$ equatorial plane (Fe-N_{eq} =1.84−2.1 Å). The fifth N atom of the $L_{222}N_5$ ligand is uncoordinated since Fe-N = 3.5 Å. Costa et al reported that this system remains LS up to 420 K, but that it undergoes light-induced excited spin-state trapping from LS (S=0) to HS (S=2) states at low temperature, by photoexcitation at 532 nm. This photoinduced HS state remains stable up to a typical temperature T(LIESST) ≈110K, as characterized by magnetic susceptibility measurements after light irradiation.[8] In addition, temperature-dependent diffuse absorption spectra of the hydrated $[Fe(L_{222}N_5)(CN)_2].H_2O$ complex, measured in the 450-850 nm range was also used to characterize the change of electronic state. The switching from LS to HS is associated with an increase of optical absorption above ≈ 640 nm and a decrease below. In the following, we exploit these spectroscopic fingerprints, to study the ultrafast photoswitching dynamics. Ababei et al. also revealed the structure of the complex in its HS state, which appears in the structure of $[(Mn(saltmen)_2Fe(L_{222}N_5)(CN)_2](ClO_4)_2\cdot 0.5CH_3OH$. In this trinuclear complex, the two [Mn(saltmen)] moieties are bridged by one $[Fe^{II}(L_{222}N_5)(CN)_2]$ brick, which is in the HS state. It was found that the HS Fe^{II} metal ion is then heptacoordinated, by 2 axial CN groups (Fe−CN = 2.17−2.18 Å) and the 5 N atoms of the macrocyclic $L_{222}N_5$ ligand (with Fe−N =2.15−2.32 Å, Fig. 1).

Here we use femtosecond optical spectroscopy, at the Institut de Physique de Rennes[9] and femtosecond X-ray absorption at the XPP station[10] of the LCLS X-ray Free Electron Laser (X-FEL) to study in real time the photoswitching dynamics of $[Fe(L_{222}N_5)(CN)_2]$ in solution. The sample was photoexcited by ≈50 fs laser pulse at different wavelengths in the [490−680] nm range (see experimental section).

[a] S. Zerdane, E. Collet, X. Dong, M. Lorenc, M. Cammarata
Univ Rennes 1, CNRS, Institut de Physique de Rennes, UMR 6251, UBL, F-35042 Rennes, France
E-mail: eric.collet@univ-rennes1.fr, marco.cammarata@univ-rennes1.fr
[b] H. F. Wang, C. Desplanches, G. Chastanet, S. F. Matar,
CNRS, Université de Bordeaux, ICMCB, 87 avenue du Dr A. Schweitzer, Pessac, F'33608, France
[c] Lebanese German University (LGU), Sahel Alam Campus, P.O.BOX 206 Jounieh. Lebanon
[c] M. Chollet, J. M. Glownia, Henrik Lemke
LCLS, SLAC National Laboratory, Menlo Park, 94025, CA, USA.
[d] H.T. Lemke, SwissFEL, Paul Scherrer Institut, Villigen PSI 5232, Switzerland

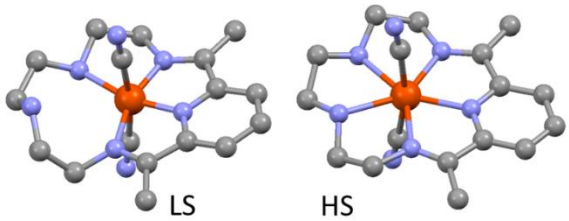

Figure 1. Structures obtained by Ababei et al,[8] in LS $[Fe(L_{222}N_5)(CN)_2]\cdot H_2O$ crystals (left) and in the complex $[(Mn(saltmen))_2Fe(L_{222}N_5)(CN)_2](ClO_4)_2\cdot 0.5CH_3OH$, where HS $[Fe(L_{222}N_5)(CN)_2]$ (right) connects two [Mn(saltmen)] units (not shown).

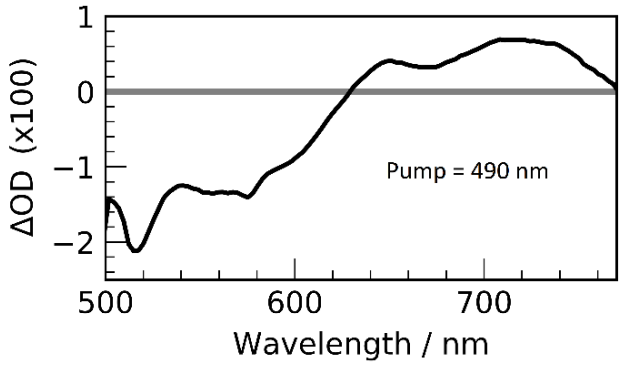

Figure 2. Variation of the optical density (ΔOD) recorded with white-light spectrometer 2 ps after photo-excitation at 490 nm. The OD increase in the IR (above ≈640 nm) and decrease in the visible parts of the spectrum is characteristic of the change from LS to HS states, as observed by LIESST experiments at low temperature.

Results and Discussion

Femtosecond optical spectroscopy was used to study the ultrafast spin-state switching dynamics of $[Fe(L_{222}N_5)(CN)_2]$ dissolved in water at room temperature. We used different pump and probe wavelengths. We measured the spectral optical density change (ΔOD) in the 500-770 nm range with white-light spectroscopy, after photoexcitation at 490 nm (≈10μJ.mm^{-2}). We show in Fig. 2 the OD change measured 2 ps after photo-excitation. The OD decrease below ≈ 640 nm (visible) and OD increase above (IR) are characteristic of the LIESST effect, also characterized by a photomagnetic experiment at low temperature,[8] and the change in figure 2 can be safely attributed photoswitching from LS to HS. Single-wavelength probe (680 nm) measurements gave more details about the switching dynamics induced by 490 nm pump (Fig. 3a). We observe two main steps: a transient peak immediately after laser excitation followed by a fast OD increase and a slower change towards a plateau on the ps timescale. These features are similar to the ones observed during LIESST in $Fe^{II}N_6$ systems with an almost octahedral coordination. The transient peak is the signature of the short-lived MLCT, which rapidly decays towards the HS state with a corresponding OD change within $\tau\approx100$ fs. The slower OD change within $\tau_{VC}\approx3$ ps corresponds to vibrational cooling in the HS potential.[3],[4] In addition, a damped oscillation at ≈ 47 cm^{-1} (710 fs period) accompanies the process. The global OD increase in IR and decrease in visible range, observed during conversion from LS to HS state on the ps timescale (Fig. 2), are also observed for photoexcitation at 530, 580 and 680 nm (Fig. 3 b-d). However, the photo-switching dynamics are different, as shown here for the OD change time traces measured at 490 nm probing wavelength for the different excitation wavelengths (Tab. 1).

We measured transient X-ray absorption change (XAS) at the Fe K edge, induced by photoexcitation at 530 nm, at the XPP station of the LCLS X-FEL. The relative change $\Delta I(t)/I_{off}$ at 7125 eV is sensitive to spin-state switching in Fe^{II} materials, including both electronic and structural contributions.[3g-i, 4e] Fig. 4 shows the $\Delta I(t)/I_{off}$ increases after photoexcitation, characteristic of the LS to HS transformation. A Transient change of opposite sign is also observed within the first 100 fs, which highlights the presence of one (or several) short-lived intermediate(s). These XAS results fingerprint the LS to HS spin-state photo-switching, accompanied by coherent oscillation (≈47 cm^{-1}).

To better understand the process, an accurate description of the initial excited states is required, and provided by DFT and time dependent DFT (TD-DFT) calculations.[11] TD-DFT lead to the natural transition orbitals (NTO), through an account for hole–particle pairs involved in the excited states induced by the pump light. TD-DFT as implemented in the Gaussian G09 package[12] was applied for obtaining the NTO of LS $[Fe(L_{222}N_5)(CN)_2]$, starting from geometry optimized molecule with UB3LYP/6-31g(d,p) functional-basis set, found to be similar to the hexacoordinated structure found by X-ray diffraction.[8] Because of the low symmetry of the molecule, the d orbitals of the Fe and the ligand orbitals are mixed. However, from Fig. 5 different types of photo-excitations can be distinguished. In the low energy excitation region, the 680 nm pump excitation corresponds well to the transition calculated at 1.91 eV. The hole has some d non-bonding character and the particle some d anti-bonding character. Both hole and particle NTOs involve the ligand. Given the low symmetry of the system, this excitation is analogous to a d-d transition (d-d excitation is forbidden in octahedral FeN_6 systems and allowed in lower symmetry systems,[13] like FeN_4O_2). We identify another type of d-d excitation at 2.12 eV (close to 580 nm). The hole has some d non-bonding character and the particle some d anti-bonding character, but the particle weight is strong on the CN groups of the ligand. Excitation around 530 nm corresponds to a transition calculated at 2.34 eV, which has a stronger metal-to-ligand charge-transfer character, with high particle weight on the macrocyclic ligand equatorial plane. In the following discussion, 680 nm excitation is referred to as d-d_1, 580 nm as d-d_2 and 530 nm as MLCT for the sake of simplicity.

To understand the nature of the oscillation observed in the photoinduced HS state, we carried G09 molecular vibration calculations in the heptacoordinated HS state. In the low frequency region, we found vibration modes at 30 cm^{-1}, 46 cm^{-1} and 52 cm^{-1}. The modes at 30 and 52 cm^{-1} correspond to ligand torsion modes.

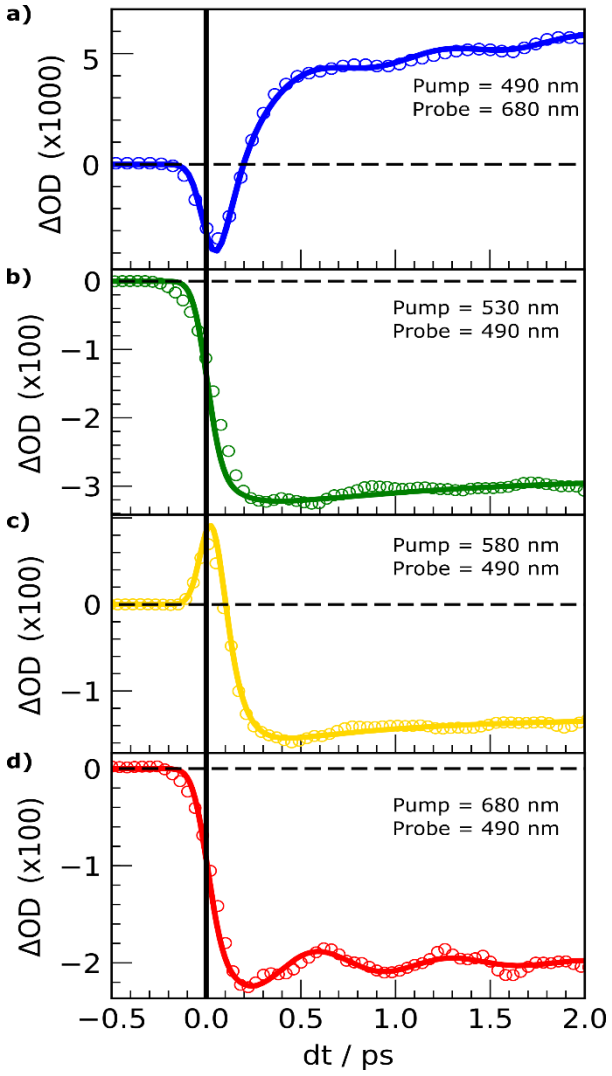

Figure 3. Kinetic traces of ΔOD at selected wavelengths obtained by two-colour pump-probe experiment at room temperature. The solid lines show the fit of the data, with a bi-exponential model describing the intermediate state, the vibrational cooling, and the coherent vibration in a and d.

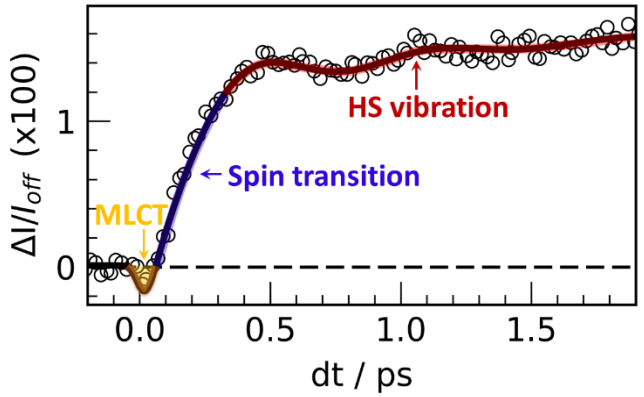

Figure 4. Time resolved change of the relative X-ray absorption $\Delta I(t)/I_{off}$ measured at 7125 eV. The fit (thick line) takes into account the spin transition with the MLCT to HS decay τ =150(10) fs and a damped oscillation with 710 fs period (47 cm^{-1}).

Table 1. Physical parameters used for the fits in Fig. 3-4. τ: LS-to-HS switching, τ_{VC}: vibrational cooling and ν: oscillation frequency.

Pump / probe	Figure	Excitation	τ (fs)	τ_{VC} (fs)	ν (cm^{-1})
490 nm / 680 nm	3a	MLCT	130 (10)	3.1 (2)	47 (1)
530 nm / 490 nm	3b	MLCT	120 (10)	1.2 (1)	-
580 nm / 490nm	3c	d-d	75 (10)	0.7 (1)	-
680 nm / 490 nm	3d	d-d	75 (10)	0.7 (1)	47 (1)
530 nm / 7125 eV	4	MLCT	150 (10)	-	47 (1)

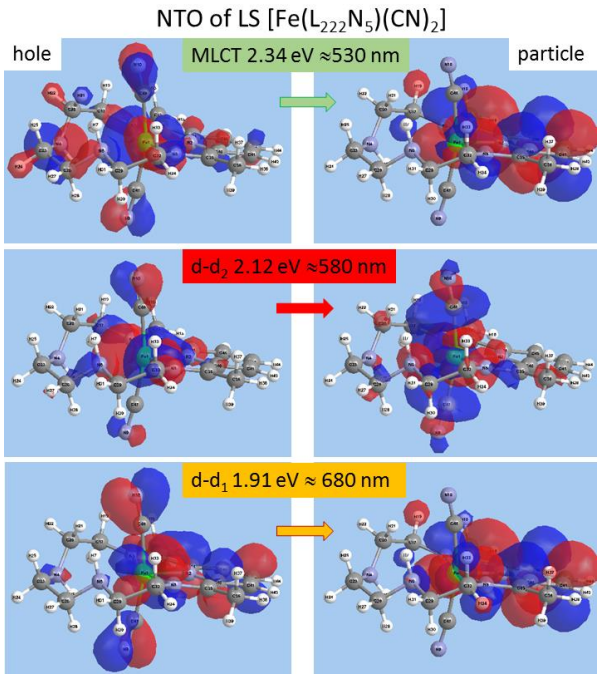

Figure 5. NTO of hole and particle for different excitation wavelengths, showing MLCT-like transition at high energy and d-d-like transitions at low energy.

Fig. 6 shows the main atomic motions for the mode calculated at 46 cm^{-1}, which is of specific interest for interpretation of the observed XANES oscillations. It corresponds to the bending of the NC-Fe-CN axis schematically indicated by the arrows showing opposite motions of Fe and CN groups. This induces small oscillation of some Fe-N bond lengths, as the macrocycle remains almost rigid in this mode. In addition, we found a stretching mode at 183 cm^{-1}, where three Fe-N bonds oscillate in phase and two remain almost constant (Fig. 6). We found another type of stretching mode at 263 cm^{-1}, with in-phase elongation of the two Fe-CN bonds perpendicular to the macrocyclic ligand.

Now a scenario can be built up to explain the experimental results. As both optical and X-ray data evidence (at least) one intermediate state, characterized with a transient peak and a fast change on the fs timescale, we use a phenomenological model to fit the data. It includes an initially photo-induced state (MLCT), which stochastically populates the final HS state where the system undergoes a damped oscillatory motion.

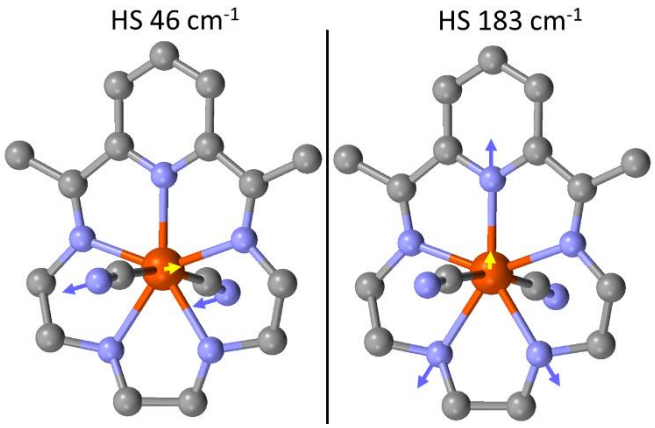

Figure 6. Representation of the vibration modes calculated at 46 cm^{-1} for the the NC-Fe-CN bending and 183 cm^{-1} for some Fe-N stretching in the heptacoordinated HS state.

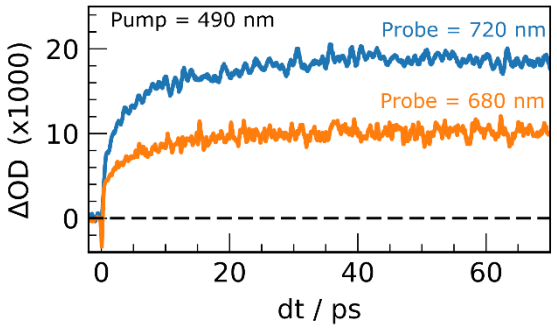

Figure 7. ΔOD time traces at 680 and 720 nm after photoexcitation at 490 nm.

This simple model, which was used for $Fe(bpy)_3^{2+}$,[3h] is applied to the present XAS data and is able to reproduce all main features of the experimental data (Fig. 4). In particular, photoexcitation at 530 nm (MLCT) creates initially a formal Fe^{3+} state. It was shown in $Fe(bpy)_3^{2+}$ that for the XAS data this change of oxidation state results in a transient negative peak at 7125 eV just after laser excitation, because of the global spectral shift by ≈ 1 eV towards higher energy of the XANES spectra of the MLCT state.[3h] The change towards the HS state (Fe^{II}), accompanied by an increase of the distance between the Fe and the neighbouring atoms is associated with an increase of XAS at 7125 eV, as reported in different systems.

The fit to the XAS time trace in Fig. 4 (& Tab. 1) indicates that the HS state is populated within 150(10) fs and that a 47 cm^{-1} molecular vibration is activated and damped with a 800 fs time constant. Since G09 calculations did not reveal molecular vibrations in the LS state below 55 cm^{-1}, we identify the mode observed as the HS 46 cm^{-1} mode found in molecular calculations (see Fig. 5). This is an indication that the HS state, with heptecoordinated structure, forms rapidly after photo-excitation, although an EXAFS study would be required to state firmly that the complex changes from hexa to heptacoordinated structures. We can also notice that optical pump-probe studies performed up to 80 ps after 490 nm excitation did not reveal slower transformation process (Fig. 7), except the vibrational cooling component (τ_{VC}≈ 1-3 ps). We analyse in a similar way the optical pump-probe data through the OD dynamical time traces shown in Fig. 3, taking also into account a vibrational cooling component. Table 1 lists the physical parameters used for the fits shown in Fig. 3. A time constant $\tau \approx 130(10)$ fs is found for excitation at 490 nm and 530 to describe the decay of the MLCT to the HS state, whereas a 75(10) fs time constant is found for lower energy excitation at 580 and 680 nm to describe the decay of the d-d excitations to the HS state, thus bypassing MLCT. We also observe different optical fingerprints of the intermediates under 530, 580 and 680 nm excitation for the same probing wavelength. Vibrational cooling varies with the probe wavelength, as it is often the case. We also observe the vibration mode at 47 cm^{-1} in Fig. 3a & 3d, but not 3b and 3c, probably because of the signal/noise limitation.

The present study provides experimental results on the LIESST dynamics in the $[Fe(L_{222}N_5)(CN)_2]$ system, with unusual ligand structure. It is then interesting to discuss similarities and differences compared to previous studies of more conventional $Fe^{II}N_6$ systems such as $Fe(bpy)_3^{2+}$, $[Fe(PM\text{-}AZA)_2(NCS)_2]$, $[Fe(phen)_2(NCS)_2]$...[3a, 3h, 4c, 4e, 4h] When these systems are in the LS state, the accessible optical excitation is the MLCT state, as d-d excitation is forbidden, or very weak, because of their almost octahedral symmetry. The main reaction coordinate responsible for their spin state trapping is the elongation of the 6 Fe-N bonds. The FeN_6 breathing mode, with in-phase oscillation of the Fe-N bonds, is then coherently activated during the structural trapping in the HS potential, giving rise to OD or XAS oscillation as the ligand field oscillate. LIESST is also accompanied by the coherent activation of other modes in the HS potential energy surface. For $[Fe(L_{222}N_5)(CN)_2]$, we find a similar time constant $\tau \approx$ 130 fs for the decay towards the HS state after MLCT excitations performed at 530 and 490 nm. However, $[Fe(L_{222}N_5)(CN)_2]$ has a molecular structure different from conventional FeN_6 systems and the structural trapping reaction coordinate is different, with a change from hexacoordinated (LS) to heptacoordinated (HS) and an elongation of the Fe-N and Fe-CN bonds. DFT calculation found HS Fe-ligand modes with Fe-N (183 cm^{-1}, 182 fs period, Fig. 6) or Fe-CN (263 cm^{-1}, 127 fs period) stretching characters, but these are different in nature from the global molecular breathing around 120 cm^{-1} (≈280 fs period) reported in FeN_6 systems. As for $[Fe(L_{222}N_5)(CN)_2]$ the decay from the MLCT to the HS state occurs within ≈ 130 fs, an important structural decoherence occurs during the inter-system crossing for the Fe-N and Fe-CN stretching modes, because their ½ period is shorter than the population time of the HS potential energy surface. These modes are consequently populated incoherently in the HS and cannot give rise to coherent oscillation of XAS or OD signal. For FeN_6 systems, the breathing mode with ≈280 fs period is observed because its half period is longer than the MLCT to HS decay. This condition of half-period longer than the MLCT decay is fulfilled in the case of $[Fe(L_{222}N_5)(CN)_2]$ for the 47 cm^{-1} mode (710 fs period) observed in Fig. 3 and 4, which is coherently populated in the HS potential. This mode modulates XAS and optical data because the associated bending of the NC-Fe-CN groups strongly modifies the local structure around the Fe and also the electronic state. Indeed, because of the sigma character of the Fe-CN bonds, the bending modifies the electronic density around the Fe. For FeN_6 systems, several low-frequency modes are also coherently activated during LIESST, as reported by optical spectroscopy.

Another interesting aspect of $[Fe(L_{222}N_5)(CN)_2]$ compared to FeN_6 systems is that the low symmetry allows optical excitation of the LS state at lower energy than the MLCT, such as d-d excitation at 680 nm. This excitation scheme was also recently discussed in $Fe(pap\text{-}5NO_2)_2$, a FeN_4O_2 ligand-field system, where intense d-d bands were used to induce LIESST.[13] Compared to MLCT excitation, this d-d excitation induces a faster decay towards the HS state and the observed 75 fs timescale is similar to the one found here for $[Fe(L_{222}N_5)(CN)_2]$. This faster decay limits the structural decoherence in the intermediate state(s), which translates in a larger oscillating signal in the final HS state under d-d compared to MLCT excitation, as observed in Fig. 3. Compared to these previous results on more conventional FeN_6 or FeN_4O_2 systems, the present study indicates that the trapping timescales of the HS state, under MLCT (≈ 130 fs) or d-d excitation (≈ 75 fs), are very similar for $[Fe(L_{222}N_5)(CN)_2]$. The different ligand structure involves however different modes in the structural trapping of the process, but only those with ½ period shorter than the population of the HS potential can be observed, and here not those with Fe-N or Fe-CN stretching character. It also should be noticed here that optical pump pulses with duration longer than the MLCT decay preclude the observation of this coherent structural dynamics, as a too long optical pumping will result in dephasing in the population of the HS state. In addition, probe pulses longer than 100 fs will decrease the time resolution, which can make the observation of coherent oscillations difficult or even preclude it. The use of 100 fs (or shorter) optical or X-ray pulses is therefore required to induce and observe coherent structural dynamics. In the present case, the main reason for the structural decoherence is intrinsic to the system and driven by the lifetime of the intermediate(s).

Conclusions

Our femtosecond optical and X-ray absorption studies show that the spin-state switching mechanism in $[Fe(L_{222}N_5)(CN)_2]$ occurs on similar timescales than in more conventional spin-crossover materials of almost octahedral symmetry. The low symmetry of $[Fe(L_{222}N_5)(CN)_2]$ allows both MLCT and d-d like photoexcitations in the LS hexacoordinated state. We found optical fingerprints of these intermediates and a faster decay from d-d to HS than from MLCT to HS, which induces a coherent structural dynamics related to the bending of the N-C-Fe-C-N group. The structural relaxation in the HS state is complex, involving a change of coordination and a large ligand reorganization. We hope that in a near future complementary X-ray-based techniques extending down to the femtosecond range[14] (including spectroscopy, scattering, and diffraction) will make it possible to map in more detail the dynamics of the electronic and structural degrees of freedom, as well as the global structural change from hexacoordinated in the LS state to heptacoordinated in the HS state. This will also help comparing more directly with X-ray the evolution of the structural dynamics as d-d and MLCT excitations induce different pathways on the potential energy surface.

Experimental Section

The complex $[Fe(L_{222}N_5)(CN)_2]$ has been synthesized as already described by Nelson[6]. In details, 1.20 g (6 mmol) of iron chloride tetrahydrate, 1 g (6 mmol) of 2,6-diacetylpyridine, and 0.1 g of sodium dithionite (used as reducing agent to remove traces of trivalent iron ion) were dissolved in 15 mL of methanol and 10 mL of water. The triethylenetetramine (0.876 g, 6 mmol) was added dropwise. The mixture was kept under nitrogen reflux at 75 °C for 16 h approximately (formation of $[Fe(L_{222}N_5)(Cl)_2]$). After filtration to remove traces of impurities, 15 mL of aqueous solution containing an excess of sodium cyanide NaCN (4g; 0.08 mol) and 0.1 g of sodium dithionite was added. This solution was then kept stirring for ca. 6 hours at room temperature. A polycrystalline powder is formed. The solid formed is then filtered and washed with 10 mL of degassed water and dried under vacuum. Finally 0.9 g (yield ~ 40%) of dark purple powder was collected. This powder was then disolved in water for ultrafast experiments.

The time resolved studies of aqueous solution of $[Fe(L_{222}N_5)(CN)_2]$ were performed at room temperature, using two complementary pump/probe techniques. For femtosecond optical pump-probe spectroscopy with ≈60 fs time resolution (RMS), different wavelengths were used for photoexcitation (490, 530, 580 and 680 nm) with similar excitation fluences (≈ 10 $\mu J.mm^{-2}$). Time-resolved OD change measurements were performed at selected wavelengths to track the photoswitching dynamics. The femtosecond optical pump-probe experiments were configured in visible-NIR transmission geometry with a quasi-collinear configuration of pump and probe beams. More details about the experimental set-up are presented in the paper by Lorenc et al.[9] The time resolved X-ray absorption signal of aqueous solution of $[Fe(L_{222}N_5)(CN)_2]$ was also measured at room temperature, using the optical pump / X-ray probe technique through total fluorescence at the X-ray Pump Probe station, LCLS.[10] Lemke et al presented the XAS experimental set-up in more details.[3] We used a C(111) double crystal monochromator to probe X-ray absorption at 7125 eV, which is known to be very sensitive to the spin state switching in FeII systems. The relative X-ray to optical pulses arrival time was recorded using the timing tool diagnostic.[15] The overall time resolution was found to be ~50 fs RMS.

Acknowledgements

Use of the Linac Coherent Light Source (LCLS), SLAC National Accelerator Laboratory, is supported by the U.S. Department of Energy, Office of Science, Office of Basic Energy Sciences under Contract No. DE-AC02-76SF00515. M.Ca. and E.C. thank ANR (ANR-13-BS04-0002 FEMTOMAT and ANR-15-CE32-0004 BioXFEL) and Centre National de la Recherche Scientifique (CNRS) (PEPS SASLELX) for financial support. Part of this work was performed in the frame of the COST action ECOSTBio. S.Z. thanks Région Bretagne for financial support (ARED 8925/XFELMAT).

Keywords: spin crossover • x-ray absorption spectroscopy • time-resolved spectroscopy • intersystem crossing • LIESST

[1] a) S. Decurtins, P. Gütlich, C. P. Köhler, H. Spiering, A. Hauser, *Chemical Physics Letters* **1984**, *105*, 1-4; b) M. A. Halcrow, *Spin-crossover materials : properties and applications*, Wiley, **2013**.
[2] A. Hauser, *Top Curr Chem* **2004**, *234*, 155-198.
[3] a) G. Aubock, M. Chergui, *Nature Chemistry* **2015**, *7*, 629-633; b) W. K. Zhang, R. Alonso-Mori, U. Bergmann, C. Bressler, M. Chollet, A. Galler, W. Gawelda, R. G. Hadt, R. W. Hartsock, T. Kroll, K. S.

Kjaer, K. Kubicek, H. T. Lemke, H. Y. W. Liang, D. A. Meyer, M. M. Nielsen, C. Purser, J. S. Robinson, E. I. Solomon, Z. Sun, D. Sokaras, T. B. van Driel, G. Vanko, T. C. Weng, D. L. Zhu, K. J. Gaffney, *Nature* **2014**, *509*, 345-348; c) J. K. McCusker, A. Vlček, *Accounts of Chemical Research* **2015**, *48*, 1207-1208; d) K. Hong, H. Cho, R. W. Schoenlein, T. K. Kim, N. Huse, *Accounts of Chemical Research* **2015**, *48*, 2957-2966; e) J. J. McGarvey, I. Lawthers, K. Heremans, H. Toftlund, *Journal of the Chemical Society, Chemical Communications* **1984**, 1575-1576; f) J. K. Mccusker, K. N. Walda, R. C. Dunn, J. D. Simon, D. Magde, D. N. Hendrickson, *Journal of the American Chemical Society* **1993**, *115*, 298-307; g) C. Bressler, C. Milne, V. T. Pham, A. ElNahhas, R. M. van der Veen, W. Gawelda, S. Johnson, P. Beaud, D. Grolimund, M. Kaiser, C. N. Borca, G. Ingold, R. Abela, M. Chergui, *Science* **2009**, *323*, 489-492; h) H. T. Lemke, K. S. Kjær, R. Hartsock, T. Brandt van Driel, M. Chollet, J. M. Glownia, S. Song, D. Zhu, E. Pace, S. F. Matar, M. N. Nielsen, M. Benfatto, K. J. Gaffney, E. Collet, M. Cammarata, *Nat. Commun.* **2017**, *8*, 15342; i) H. T. Lemke, C. Bressler, L. X. Chen, D. M. Fritz, K. J. Gaffney, A. Galler, W. Gawelda, K. Haldrup, R. W. Hartsock, H. Ihee, J. Kim, K. H. Kim, J. H. Lee, M. M. Nielsen, A. B. Stickrath, W. K. Zhang, D. L. Zhu, M. Cammarata, *Journal of Physical Chemistry A* **2013**, *117*, 735-740; j) S. E. Canton, X. Y. Zhang, L. M. L. Daku, A. L. Smeigh, J. X. Zhang, Y. Z. Liu, C. J. Wallentin, K. Attenkofer, G. Jennings, C. A. Kurtz, D. Gosztola, K. Warnmark, A. Hauser, V. Sundstrom, *Journal of Physical Chemistry C* **2014**, *118*, 4536-4545.

[4] a) R. Bertoni, M. Lorenc, H. Cailleau, A. Tissot, J. Laisney, M. L. Boillot, L. Stoleriu, A. Stancu, C. Enachescu, E. Collet, *Nat Mater* **2016**, *15*, 606-610; b) R. Bertoni, M. Lorenc, T. Graber, R. Henning, K. Moffat, J. F. Létard, E. Collet, *Crystengcomm* **2016**, *18*, 7269-7275; c) R. Bertoni, M. Cammarata, M. Lorenc, S. F. Matar, J. F. Letard, H. T. Lemke, E. Collet, *Acc Chem Res* **2015**, *48*, 774-781; d) R. Bertoni, M. Lorenc, A. Tissot, M. L. Boillot, E. Collet, *Coordination Chemistry Reviews* **2015**, *282-283*, 66-76; e) M. Cammarata, R. Bertoni, M. Lorenc, H. Cailleau, S. Di Matteo, C. Mauriac, S. F. Matar, H. Lemke, M. Chollet, S. Ravy, C. Laulhe, J. F. Letard, E. Collet, *Physical Review Letters* **2014**, *113*, 227402; f) R. Bertoni, M. Lorenc, A. Tissot, M. Servol, M. L. Boillot, E. Collet, *Angew Chem Int Ed Engl* **2012**, *51*, 7485-7489; g) E. Collet, N. Moisan, C. Balde, R. Bertoni, E. Trzop, C. Laulhe, M. Lorenc, M. Servol, H. Cailleau, A. Tissot, M. L. Boillot, T. Graber, R. Henning, P. Coppens, M. Buron-Le Cointe, *Phys Chem Chem Phys* **2012**, *14*, 6192-6199; h) A. Marino, M. Cammarata, S. F. Matar, J.-F. Létard, G. Chastanet, M. Chollet, J. M. Glownia, H. T. Lemke, E. Collet, *Structural Dynamics* **2016**, *3*, 023605; i) A. Marino, M. Buron-Le Cointe, M. Lorenc, L. Toupet, R. Henning, A. D. DiChiara, K. Moffat, N. Brefuel, E. Collet, *Faraday Discuss* **2015**, *177*, 363-379; j) A. Marino, P. Chakraborty, M. Servol, M. Lorenc, E. Collet, A. Hauser, *Angewandte Chemie-International Edition* **2014**, *53*, 3863-3867.

[5] M. Cammarata, K. Y. Lin, J. Pruet, H. W. Liu, J. Brodbelt, *Anal Chem* **2014**, *86*, 2534-2542.

[6] S. M. Nelson, P. D. A. McIlroy, C. S. Stevenson, E. Konig, G. Ritter, J. Waigel, *Journal of the Chemical Society, Dalton Transactions* **1986**, 991-995.

[7] R. Ababei, C. Pichon, O. Roubeau, Y. G. Li, N. Brefuel, L. Buisson, P. Guionneau, C. Mathoniere, R. Clerac, *J Am Chem Soc* **2013**, *135*, 14840-14853.

[8] J. S. Costa, C. Balde, C. Carbonera, D. Denux, A. Wattiaux, C. Desplanches, J.-P. Ader, P. Gütlich, J.-F. Létard, *Inorganic Chemistry* **2007**, *46*, 4114-4119.

[9] M. Lorenc, C. Balde, W. Kaszub, A. Tissot, N. Moisan, M. Servol, M. Buron-Le Cointe, H. Cailleau, P. Chasle, P. Czarnecki, M. L. Boillot, E. Collet, *Physical Review B* **2012**, *85*.

[10] M. Chollet, R. Alonso-Mori, M. Cammarata, D. Damiani, J. Defever, J. T. Delor, Y. Feng, J. M. Glownia, J. B. Langton, S. Nelson, K. Ramsey, A. Robert, M. Sikorski, S. Song, D. Stefanescu, V. Srinivasan, D. Zhu, H. T. Lemke, D. M. Fritz, *Journal of Synchrotron Radiation* **2015**, *22*, 503-507.

[11] R. L. Martin, *The Journal of Chemical Physics* **2003**, *118*, 4775-4777.

[12] M. J. e. a. Frisch, *Gaussian, Inc., Wallingford CT* **2016**.

[13] S. Zerdane, L. Wilbraham, M. Cammarata, O. Iasco, E. Rivière, M. L. Boillot, I. Ciofini, E. Collet, *Chem. Sci.* **2017**, *8*, 4978-4986.

[14] M. Chergui, E. Collet, *Chemical Reviews* **2017**, *117*, 11025-11065.

[15] M. Harmand, R. Coffee, M. R. Bionta, M. Chollet, D. French, D. Zhu, D. M. Fritz, H. T. Lemke, N. Medvedev, B. Ziaja, S. Toleikis, M. Cammarata, *Nature Photonics* **2013**, *7*, 215-218.